Integrated Estimation/Identification Using Second-Order Dynamic Models

John L. Crassidis*

D. Joseph Mook†

Abstract

An algorithm is presented which accurately identifies multi-input-multi-output systems characterized by vibrating structures. More specifically, an identification technique is integrated with an optimal estimator in order to develop an algorithm which is robust with respect to measurement and process noise. The unique functional form of the integrated approach utilizes systems described by second-order models. Therefore, theoretical mass, damping, and stiffness matrices, associated with lumped parameter models, are tailored with experimental time-domain data for system estimation and identification. This leads to an algorithm that is computational efficient, producing realizations of complex multiple degree-of-freedom systems. The combined estimation/identification algorithm is used to identify the properties of an actual flexible truss from experimental data. Comparison of experimental frequency-domain data to the predicted model characteristics indicates that the integrated algorithm produces near minimal realizations coupled with accurate modal properties.

Introduction

Combining theoretical models with experimental data is an important aspect for both system identification and estimation. More specifically, estimation techniques utilize past observations to estimate response characteristics which generally minimize the expectation of the square of the error between the actual measurements and the estimated signal. Common linear estimation algorithms include, the Weiner filter (Weiner, 1949), maximum likelihood techniques (Iliff et al, 1984), and least square techniques (Bode and Shannon, 1950). The Kalman filter (Kalman, 1960) expands the Weiner problem by incorporating state-space formulations in the filter design. This algorithm, along with its

* National Research Council Postdoctoral Fellow, NASA-Goddard Space Flight Center, Guidance and Control Branch Code 712, Greenbelt MD 20771.
† Associate Professor, Department of Mechanical and Aerospace Engineering, Member ASME. State University of New York at Buffalo, Buffalo NY, 14260.

derivatives, not only filters noisy measurements, but provides state estimates of the physical system. Also, the Kalman filter algorithm can be expanded for systems described by linear second-order matrix equations (Hashemipour and Laub, 1988). This is extremely useful in the study of vibrational problems such as large space structures.

Time domain techniques are useful in identifying the modal properties of a flexible structure. Realized state-space models can be used for various control designs such as, LQR, LQG, and/or H_∞ algorithms. A few identification algorithms of particular interest include, AutoRegressive Moving Average (ARMA) models (Astrom and Eykhoff, 1971), Least Square algorithms (Smith, 1981), the Impulse Response technique (Yeh and Yang, 1987), the Polyreference method (Leuridan and Vold, 1983), and Ibrahim's Time Domain (Ibrahim and Mikulcik, 1977) technique. The Eigensystem Realization Algorithm (Juang and Pappa, 1985) expands upon these algorithms by utilizing singular value decompositions in order to better identify physical modes from time domain measurements. In most circumstances, the identification of SISO models from experimental data can easily be obtained. However, since transmission zeros impose strict mathematical constraints on system matrices, *minimal* realizations of MIMO systems are usually difficult to obtain experimentally. Possible sources of error include: sensor and instrumentation noise, slight nonlinearities inherent in the structure, and/or background vibration. Therefore, for system identification of flexible structures, multiple experiments are usually performed in order to improve mathematical models. However, this requires extensive computational time and effort.

In recent years several techniques have been developed which expand upon analytical models to conform with experimental data. In particular, finite-element models of a given structure are compared with experimentally measured data in order to update second-order models (see, e.g. "Heylen, 1990," and "Minas and Inman, 1990"). The experimental data is usually in the form of modal data, such as natural frequencies, damping ratios, and modes shapes. In almost all circumstances the modal data is incomplete since measurements are usually taken along a limited number of selected locations. This increases the complexity of updating analytical models, since finite-element models are generally of larger order than the experimentally measured modes (Heylen, 1990). In the case of MIMO models,

the complexity of finite-element updating increases since accurate (symmetric) positive definite stiffness and positive semi-definite damping matrices are usually not guaranteed to have the same physical significance as the original modeling (Minas and Inman, 1990). Also, several iterations of the modified system matrices are usually required in order to achieve satisfactory results.

The identification algorithm developed in this paper identifies accurate (near minimal) state-space realizations of a structure from only one set of experimental data. This algorithm combines an optimal state estimation routine, known as the Minimum Model Error (MME) estimator (Mook and Junkins, 1988), with the Eigensystem Realization Algorithm (ERA) in order to provide robust features for MIMO identification. The advantages of the MME estimator are: (i) the model error is assumed unknown and is estimated as part of the solution; (ii) the model error may take any form including nonlinear; and (iii) the algorithm is robust in the presence of high measurement noise. Therefore, accurate state estimates can be obtained and used during the identification process.

The combined MME/ERA identification algorithm has been successfully applied to numerous applications (see, e.g. "Roemer and Mook, 1990" and "Mook and Lew, 1988"). Recent work by Roemer and Mook (1992) utilized this algorithm to identify the modal properties of damped structures using measurements with a high noise content. However, only modal properties (natural frequencies and damping ratios) of SISO systems were considered. Also, only smoothing of output measurements was applied. No state estimation information was used during the identification process. The implementation in this paper is to expand the MME/ERA algorithm by utilizing the second-order model form together with state estimate information. The benefits of second-order models over first-order forms include: an increase in the computational efficiency, physical insight of modal properties are retained, and more accurate model realizations of actual systems are possible. Also, transforming second-order models to first-order form destroys the sparsity of the structural mass, damping, and stiffness matrices (Juang and Phan, 1992). By utilizing second-order models in the MME estimator, the inherent minimal MIMO form is retained during the identification process. Therefore, finite-element models combined with experimental data can be used as a basis for accurate (near minimal) realizations.

The organization of this paper proceeds as follows. First, the model form of a linear damped

multiple-degree-of-freedom system is presented. Then, the closed-form solution of the MME estimator is shown for linear time-invariant models. The result involves the solution of a standard Riccati equation and two sets of linear differential equations. The MME estimator is next derived for systems described by second-order models. The MME estimator is the combined with an expanded version of the ERA in order identify models accurately. Finally, the combined algorithm is used to experimentally develop a realization of an actual flexible structure. Results are shown and compared with experimental data.

Analytical Model

The structure of the physical system is assumed to be modeled by a linear proportional damped multiple-degree-of-freedom system. For vibration analysis of flexible structures two set of linear, constant coefficient, ordinary differential equations are used:

$$M\underline{\ddot{q}}(t) + D\underline{\dot{q}}(t) + K\underline{q}(t) = \tilde{B}\,\underline{u}(t) \tag{1a}$$

$$\underline{y} = H_1\underline{q}(t) + H_2\underline{\dot{q}}(t) \tag{1b}$$

where $\underline{q}$ is an $(n \times 1)$ displacement vector, M, D, and K, are mass, damping, and stiffness matrices, respectively, and H_1 and H_2 are $(q \times n)$ output matrices. The mass and stiffness matrices are assumed to be symmetric, positive definite matrices, and the damping matrix is assumed to be symmetric, positive semi-definite (Inman, 1989). The analytical mass, and stiffness matrices can be obtained by a finite-element analysis of the structure. The damping matrix is assumed to be proportional to the mass and stiffness matrices. Also, acceleration measurement output can be solved in terms displacement, velocity, and control force (i.e., direct transmission).

Since proportional damping is assumed, i.e. $KM^{-1}D = DM^{-1}K$, the system in Equation (1) can be decoupled by the modal matrix (S_m) of K, normalized with respect to the mass matrix (Inman, 1989):

$$\ddot{\underline{r}}_i(t) + 2\zeta_i\omega_i\dot{\underline{r}}_i(t) + \omega_i^2\underline{r}_i(t) = S_m^T\tilde{B}\,u(t) \tag{2}$$

where $\underline{r} = S_m^{-1}\underline{q}$, and ω_i and ζ_i are the undamped modal frequencies and modal damping ratios at the i^{th} component, respectively. Therefore, the mass, damping, and stiffness matrices from Equation (1) can be converted to diagonal modal (decoupled) matrices:

$$M_\lambda = I_{n\times n} \tag{3a}$$

$$C_\lambda = \mathrm{diag}\left[\omega_i^2\right] \tag{3b}$$

$$D_\lambda = \mathrm{diag}[2\zeta_i\omega_i] \tag{3c}$$

The state-space representation of Equation (1) is given by:

$$\begin{bmatrix}\dot{\underline{q}}\\ \ddot{\underline{q}}\end{bmatrix} = \begin{bmatrix}0_{n\times n} & I_{n\times n}\\ -M^{-1}K & -M^{-1}D\end{bmatrix}\begin{bmatrix}\underline{q}\\ \dot{\underline{q}}\end{bmatrix} + \begin{bmatrix}0_{n\times p}\\ M^{-1}\tilde{B}\end{bmatrix}u(t) \tag{4a}$$

$$y = [H_1 \quad H_2]\begin{bmatrix}\underline{q}\\ \dot{\underline{q}}\end{bmatrix} \tag{4b}$$

The state-space approach is useful for control and estimation applications. However, transforming to first-order form increases the dimension of the problem. The next section utilizes the qualities of second-order modeling in order to simplify the estimation and identification process.

Minimum Model Error Estimator

In this section, the MME algorithm is briefly reviewed for the case of linear time-invariant state-space models. See Mook and Junkins (1988) for a more detailed derivation of the algorithm. The MME algorithm assumes that the state estimates are given by a nominal (pre-specified) model and an un-modeled error vector, shown as:

$$\begin{aligned}\dot{\hat{\underline{x}}}(t) &= A_m\,\hat{\underline{x}}(t) + B_m u(t) + \underline{d}(t)\\ \hat{\underline{y}}(t) &= C_m\,\hat{\underline{x}}(t) + D_m u(t)\end{aligned} \tag{5}$$

where A_m, B_m, C_m, D_m are time-invariant nominal state matrices from the finite-element model, $u(t)$

is a $(p \times 1)$ known forcing input, $\underline{d}(t)$ is an $(2n \times 1)$ un-modeled (to-be-determined) model error vector, $\underline{\hat{x}}(t)$ is the $(2n \times 1)$ state estimate vector, and $\underline{\hat{y}}(t)$ is the $(q \times 1)$ estimated output. State-observable discrete measurements are assumed for Equation (5) in the following form:

$$\underline{\tilde{y}}(t_k) = \underline{g_k}(\underline{x}(t_k), t_k) + \underline{\nu_k} \tag{6}$$

where $\underline{\tilde{y}}(t_k)$ is an $(q \times 1)$ measurement vector at time t_k, $\underline{g_k}$ is an accurate model of the measurement process, and $\underline{\nu_k}$ represents measurement noise. The measurement noise process is assumed to be a zero-mean, Gaussian distributed process of known covariance, R.

In the MME, the optimal state estimates are determined on the basis that the measurement-minus-estimate error covariance matrix must match the measurement-minus-truth error covariance matrix. This condition is referred to as the "covariance constraint", approximated by:

$$\left\{ \left[\underline{\tilde{y}}(t_k) - \underline{\hat{y}}(t_k)\right] \left[\underline{\tilde{y}}(t_k) - \underline{\hat{y}}(t_k)\right]^T \right\} \approx R \tag{7}$$

Therefore, the output is required to fit the actual measurements with approximately the same error covariance as the actual measurements fit the truth.

A cost functional, consisting of the weighted sum square of the measurement-minus-estimate residuals plus the weighted sum square of the model correction term, is next minimized:

$$J = \sum_{k=1}^{k_{tot}} \left\{ \left[\underline{\tilde{y}}(t_k) - \underline{\hat{y}}(t_k)\right]^T R^{-1} \left[\underline{\tilde{y}}(t_k) - \underline{\hat{y}}(t_k)\right] \right\} + \int_{t_0}^{t_f} \underline{d}(\tau)^T W \underline{d}(\tau)\, d\tau \tag{8}$$

where k_{tot} is the total number of measurement points, and W is a weight matrix determined by satisfying the covariance constraint. If the measurement residual covariance is larger than R, then the measurement estimate is not close to the actual system measurements. Therefore, W should be decreased in order to

less penalize the model correction ($\underline{d}(t)$). However, if the estimate covariance is to low, then W should be increased in order to allow more model correction. The model error corrects the finite-element model in order to estimate the output using experimental measurements. Therefore, the model error term tends to update the states from the finite-element model in order to conform to actual system responses.

The necessary conditions for the minimization of J, with respect to the model correction term $\underline{d}(t)$, leads to the following Two-Point-Boundary-Value-Problem TPBVP (see Mook and Junkins, 1988):

$$\dot{\hat{\underline{x}}}(t) = A_m\,\hat{\underline{x}}(t) + B_m\,\underline{u}(t) + \underline{d}(t) \tag{9a}$$

$$\dot{\underline{\lambda}}(t) = -A_m^T\,\underline{\lambda}(t) \tag{9b}$$

$$\underline{d}(t) = -\frac{1}{2}\,W^{-1}\,\underline{\lambda}(t) \tag{9c}$$

$$\underline{\lambda}(t_k^+) = \underline{\lambda}(t_k^-) + 2\,C_m^T R^{-1}\left[\underline{\tilde{y}}(t_k) - \underline{\hat{y}}(t_k)\right] \tag{9d}$$

where $\underline{\lambda}(t)$ is a vector of co-states (Lagrange multipliers). Also, the co-state equation is updated at each measurement interval. The boundary conditions are selected such that either $\underline{\lambda}(t_0^-) = \underline{0}$ or $\underline{x}(t_0)$ is specified for the initial time and either $\underline{\lambda}(t_f^+) = \underline{0}$ or $\underline{x}(t_f)$ is specified at the final time. The solution of the TPBVP involves the determination of a linear Riccati equation and a linear differential equation.

Riccati solutions are useful in determining optimal trajectories for the design of linear control systems with quadratic cost functionals. The application of this method is expanded in order to derive matrix Riccati solutions for the MME algorithm, which includes discrete updates in the co-state equation. The co-state equation is a linear function with respect to the state estimates, given as:

$$\underline{\lambda}(t) = P(t)\,\hat{\underline{x}}(t) + \underline{h}(t) \tag{10}$$

where $P(t)$ is an $(2n \times 2n)$ homogeneous matrix and $\underline{h}(t)$ is an $(2n \times 1)$ linear inhomogeneous vector. By differentiating Equation (10) with respect to time and substituting into Equation (9a-c), the following two equations are developed:

$$\dot{P}(t) = -P(t)\,A_m + \frac{1}{2}\,P(t)\,W^{-1}P(t) - A_m^T\,P(t) \tag{11a}$$

$$\dot{\underline{h}}(t) = \left[\frac{1}{2}\,P_{ss}\,W^{-1} - A_m^T\right]\underline{h}(t) - P_{ss}\,B_m\,u(t) \tag{11b}$$

The new update equations are also derived by substituting Equation (10) into the update co-state equation in Equation (9d). Realizing that the coefficient for the state trajectory must vanish yields the two update equations:

$$P\left(t_k^-\right) = P\left(t_k^+\right) + 2\,C_m^T\,R^{-1}\,C_m \tag{12a}$$

$$\underline{h}\left(t_k^-\right) = \underline{h}\left(t_k^+\right) + 2\,C_m^T\,R^{-1}\left[D_m\,u(t_k) - \underline{\tilde{y}}(t_k)\right] \tag{12b}$$

with boundary conditions of $P\left(t_f^+\right) = 0$, $\underline{h}\left(t_f^+\right) = \underline{0}$ and $\underline{x}(t_0)$ specified. The discrete update equation for the Riccati type solution in Equation (11a) has a constant update at each measurement time. However, the solution does indeed reach steady-state values for time-invariant state-space model matrices. An approximation to the steady-state homogeneous Riccati is obtained by converting the continuous/discrete update form, given by Equations (11a) and (12a), into a completely continuous-time Riccati equation with the inclusion of sampling rate, given by:

$$P_{ss}\,A_m - \frac{1}{2}P_{ss}\,W^{-1}\,P_{ss} + A_m^T\,P_{ss} + 2\,C_m^T\,R^{-1}\,C_m/\Delta t = 0 \tag{13}$$

This approximation is fairly accurate if the sampling rate is much faster than the highest frequency present in the system dynamics (i.e., at least twice the Nyquist frequency). The solution of the steady-state Riccati gain in Equation (13) is well known (Vaughan, 1970) and is determined from an eigenvector analysis of the Hamiltonian matrix:

$$H = \begin{bmatrix} A_m & \left(-\frac{1}{2}W^{-1}\right) \\ \left(-2\,C_m^T\,R^{-1}\,C_m/\Delta t\right) & -A_m^T \end{bmatrix} \tag{14}$$

The eigenvectors of this Hamiltonian matrix are then partitioned with respect to the $(2n)$ stable and $(2n)$ unstable eigenvalues.

$$V = \begin{bmatrix} V_{11} & V_{12} \\ V_{21} & V_{22} \end{bmatrix} \tag{15}$$

where V_{11} and V_{21} correspond to the stable eigenvalues, and V_{12} and V_{22} correspond to the unstable eigenvalues. The steady-state solution is given using the eigenvectors corresponding to the stable eigenvalues:

$$P_{ss} = V_{11}\, V_{21}^{-1} \tag{16}$$

The solution for the optimal state estimates is first derived by integrating the inhomogeneous linear differential equation in Equation (11b) backwards, accounting for the discrete updates at each measurement point, given by Equation (12b). The Riccati trajectories are then stored and the optimal state equations are integrated forward:

$$\dot{\hat{\underline{x}}}(t) = \left[A_m - \frac{1}{2} W^{-1} P_{ss}\right] \hat{\underline{x}}(t) - \frac{1}{2} W^{-1} \underline{h}(t) + B_m\, u(t) \tag{17}$$

Therefore, once the steady-state homogeneous Riccati equation is solved, the solution to the standard MME problem involves solving $(4n)$ ordinary linear differential equations, given by Equation (17) and by Equation (11b), with discrete updates shown by Equation (12b).

The MME estimator is able to provide state estimates of a system using first-order form models. However, using the properties of second-order dynamic models simplifies the estimation process. This is accomplished by using the modal form system shown in Equation (3). Substituting the modal matrices into Equation (13) and partitioning the Riccati matrix yields the following:

$$\begin{bmatrix} P_{11} & P_{12} \\ P_{12} & P_{22} \end{bmatrix} \begin{bmatrix} 0_{n\times n} & I_{n\times n} \\ -(M^{-1}K) & -(M^{-1}D) \end{bmatrix} - \frac{1}{2} \begin{bmatrix} P_{11} & P_{12} \\ P_{12} & P_{22} \end{bmatrix} \begin{bmatrix} 0_{n\times n} & 0_{n\times n} \\ 0_{n\times n} & \tilde{W}^{-1} \end{bmatrix} \begin{bmatrix} P_{11} & P_{12} \\ P_{12} & P_{22} \end{bmatrix}$$

$$+ \begin{bmatrix} 0_{n\times n} & -(M^{-1}K) \\ I_{n\times n} & -(M^{-1}D) \end{bmatrix} \begin{bmatrix} P_{11} & P_{12} \\ P_{12} & P_{22} \end{bmatrix} + 2 \begin{bmatrix} H_1^T \\ H_2^T \end{bmatrix} R^{-1} [H_1 \quad H_2]/\Delta t = \begin{bmatrix} 0_{n\times n} & 0_{n\times n} \\ 0_{n\times n} & 0_{n\times n} \end{bmatrix} \tag{18}$$

Since velocity states of the model matrix (A_m) are perfect derivatives of position states, the weighting matrix (W) is partitioned to a right lower-half dominant matrix ($\tilde{W}$). Therefore, the upper left ($n \times n$) elements of the weighting matrix are zero. Also, only diagonal weighting matrices are considered (i.e. no cross-correlation weighting of states is assumed). Therefore, the weighing matrix is reduced to an ($n \times n$) matrix. Expanding Equations (17) and (18) yields the following two Riccati equations and model equation:

$$-P_{12}(M^{-1}K) - 0.5P_{12}\tilde{W}^{-1}P_{12} - (M^{-1}K)P_{12} + 2H_1^T R^{-1} H_1/\Delta t = 0_{n\times n} \tag{19a}$$

$$-P_{22}(M^{-1}D) - 0.5P_{22}\tilde{W}^{-1}P_{22} - (M^{-1}D)P_{22} + 2\Big(P_{12} + H_2^T R^{-1} H_2/\Delta t\Big) = 0_{n\times n} \tag{19b}$$

$$M\underline{\hat{\dot{q}}} + \Big[D + 0.5\Big(M\tilde{W}^{-1}P_{22}\Big)\Big]\underline{\hat{\dot{q}}} + \Big[K + 0.5\Big(M\tilde{W}^{-1}P_{12}\Big)\Big]\underline{\hat{q}} = -0.5M\tilde{W}^{-1}\underline{h}_2 + \tilde{B}\,u \tag{20a}$$

$$\underline{\hat{y}} = H_1\underline{\hat{q}} + H_2\underline{\hat{\dot{q}}} \tag{20b}$$

where $\underline{h}_2$ is the n lower-half vector of $\underline{h}$ (i.e., $\underline{h} = [\underline{h}_1 \quad \underline{h}_2]^T$) Therefore, only two ($n \times n$) algebraic Riccati equations are required for the MME estimation algorithm using second-order models. This greatly increases the computational efficiency for modeling high-order systems, as compared to using a first-order state-space form. Also, the output estimates, given by Equation (20b), are linear combinations of the state estimates, given by Equation (20a). Therefore, the output estimates of the MME algorithm help ensure that a minimal (or near minimal) MIMO system realization of a complex structure is obtained during the identification process.

Modified Eigensystem Realization Algorithm

The ERA method is a modal synthesis technique based on the concept of singular value decomposition (see "Juang and Pappa, 1985" for more details). This procedure is capable of accurately identifying the model properties of systems involving perfect or low-noise measurements. In this section the ERA is expanded to include the state and output estimates given by the MME estimator.

Consider the discrete-time linear dynamic equation:

$$\begin{aligned} \underline{x}(k+1) &= A\,\underline{x}(k) + B\,\underline{u}(k) \\ y(k) &= C\,\underline{x}(k) \end{aligned} \tag{21}$$

where $\underline{x}$ is a $(2n\times 1)$ state vector, $\underline{u}$ is a $(p\times 1)$ input vector, y is a $(q\times 1)$ output vector; and A, B, and C are $(2n\times 2n)$, $(2n\times p)$ and $(q\times 2n)$ constant matrices, respectively. A solution to Equation (21) is given by the Markov parameters from a unit impulse response:

$$Y(k) = CA^{k-1}B \qquad X(k) = A^{k-1}B \tag{22}$$

The first step in the modified ERA is to form an $(r\times s)$ block Hankel matrix composed of the impulse response data from the MME algorithm:

$$H(0) = \begin{bmatrix} Z(1) & \cdots & Z(s) \\ \vdots & \ddots & \vdots \\ Z(r) & \cdots & Z(r+s-1) \end{bmatrix} \tag{23a}$$

$$= \begin{bmatrix} \begin{bmatrix} C \\ I \end{bmatrix} \\ \begin{bmatrix} CA \\ A \end{bmatrix} \\ \vdots \\ \begin{bmatrix} CA^{r-1} \\ A^{r-1} \end{bmatrix} \end{bmatrix} \tag{23b}$$

$$[B \quad AB \quad \cdots \quad A^{s-1}B] = V_r W_s \tag{23c}$$

where r and s are arbitrary integers satisfying the inequalities $rq \geq 2n$ and $sp \geq 2n$, and l_i $(i = 1, 2, \ldots, r-1)$ and m_j $(j = 1, 2, \ldots, s-1)$ are arbitrary integers. The matrix Z consists of

the estimated output *and* estimated states given by the MME estimator, i.e. $\underline{z} = [\hat{y} \quad \hat{\underline{x}}]^T$. Therefore, state information as well as output estimates are also used during the identification process. The state information used in the ERA allows for an accurate MIMO realization with fewer experimental test runs of the actual structure.

The singular value decomposition of H may be expressed as $H = PD_nQ$. The ERA then forms the discrete-time, reduced-order model realization of dimension $2n$ in the following form:

$$\begin{aligned} A &= D_n^{-1/2} P_n^T H(\mathbf{1}) Q_n D_n^{-1/2} \\ B &= D_n^{1/2} Q_n^T E_p \\ C &= E_q^T P_n D_n^{1/2} \end{aligned} \tag{24}$$

where P_n and Q_n are formed from the first $2n$ columns of P and Q from the singular value decomposition, and D_n is the diagonal matrix of singular values. E_p^T is $[I_m, 0]$, and E_q^T is $[I_q, 0]$, where I_p and I_q are identity matrices of order p and q, respectively, and 0 is the zero matrix. Also, $H(1)$ is formed using the next time-step in Equation (23a).

The modal damping ratios and damped natural frequencies are calculated by observing the real and imaginary parts of the eigenvalues, after a transformation from the z–plane to the s–plane is completed (Juang and Pappa, 1985). The physical mode shapes are determined using the realized eigenvectors (Φ) of the ERA state matrices. The physical mode shapes are given by $\Psi = C_m \Phi$. Physical state matrices can be determined by using this mode shape matrix and the continuous eigenvalue matrix:

$$A_m = \Psi [\Lambda] \Psi^{-1} \qquad B_m = \Psi \begin{bmatrix} \frac{e^{\lambda_1 \Delta t}}{\lambda_1} & 0 & \cdots & 0 \\ 0 & \ddots & & 0 \\ \vdots & & \ddots & \vdots \\ 0 & 0 & \cdots & \frac{e^{\lambda_n \Delta t}}{\lambda_n} \end{bmatrix}^{-1} \Psi^{-1} B \tag{25}$$

where Λ is the continuous eigenvalue matrix, derived from a discrete to continuous eigenvalue transformation of the ERA state matrix. Therefore, an identification of system parameters is possible by using the physical state matrices shown in Equation (25).

Experimental Implementation

In this section, the combined MME/ERA algorithm is used to develop a MIMO realization of an actual testbed structure, shown in Figure 1. The structure consists of 39 elements connected at 18 nodes. All but two of the structural members are made from thin-walled circular aluminum tubing with an outer diameter of 0.25″ and a wall thickness of 0.05″. Each member is pinned and bolted into the nodes to eliminate looseness in the joints. Also, the frame is configured in a planar fashion so that the only significant deformation occurs perpendicular to the structure. Two of the structural members are flat aluminum bars layered with piezoceramics. Either of these struts can excite the frame since a voltage applied across the piezoceramics produces a moment on the frame. The strut on the bottom of the frame has four ceramics glued to it and serves as the control actuator. The other flat strut is configured with the same number of piezoceramics and acts as a disturbance source. Each of these active members has a thickness of 0.25″ and a width of 1.0625″. The piezoceramics are Model G-1195 from Piezo Electric Products with dimensions 2.5″ × 0.75″ × 0.01″. The sensor is a Philtec (model 88NE3) optical displacement sensor placed near node 15 or 18 at the free end of the frame. This sensor is non-colocated with both the control actuator and the disturbance source. Frequency analysis and data acquisition are performed using a Tektronix 2630 Fourier Analyzer. A more detailed description of the experimental hardware and setup can be found in Leo and Inman (1992).

Figure 1 Flexible Frame Testbed

Combined Realization Algorithm

A block diagram illustrating the steps of the robust realization algorithm is shown in Figure 2. First, the finite-element model is used as the assumed model in the MME estimator. Next, the MME estimation problem is solved. The parameters of the optimal weighting matrix are determined by using a simple gradient optimization routine with a quadratic form of the covariance constraint as a cost function. The continuous estimated state histories produced from the MME are then re-sampled. Finally, these estimated time histories are processed in order to realize an accurate model of the system parameters, using the modified version of the ERA. These steps may be repeated if necessary in order to further

smooth the measurements and improve the identification process. However, accurate identification results for this testbed required only one iteration through the MME estimation process.

Figure 2 Block Diagram of the Combined Realization Algorithm

An estimate of the noise variance from the measured data is first required in order to implement the MME estimator. The estimate is obtained by investigating the nature and magnitude of the random disturbances detected by the optical displacement sensor, while the structure is at rest. Possible disturbances include ground motions, and/or instrumentation noise. A study by Roemer and Mook (1992) indicates that if the measurement error variance is assumed to be lower than the true measurement error variance, then the estimate will never be worse than the measurements themselves. Therefore, a conservative estimate is to predict a measurement noise variance slightly lower than the "actual" covariance.

A plot of a typical output response of the structure to a random input is shown in Figure 3. The random input is applied approximately at the two second time point. The noise levels (depicted between 0 and 2 seconds) account for a substantial portion of the output time history. This makes the identification of an accurate model from raw measurements extremely difficult. According to the Central Limit Theorem (Freund and Walpole, 1987), the noise characteristics of large measurement sequences are approximately Gaussian. Therefore, from Figure 3, a predicted noise variance of approximately 1×10^{-5} (volts) is used. Results from several other test runs indicate that this variance is conservative over all measurement output nodes. Therefore, noise variances for different magnitude inputs (such as impulse responses) are normalized with respect to this predicted variance.

Figure 3 Output Response of Node 18 to a Random Input

The combined MME/ERA algorithm enables the realization of a MIMO model in the presence of significant model error, process noise, and measurement noise. In order to obtain impulse response data, the test structure is excited using a random input with a bandwidth of 0–50 Hz. An inverse and regular Fourier transformation is applied on this data to obtain the impulse response time histories. Also, only one set of data for each input is taken for the identification. Therefore, extensive and repetitive computational analysis is attenuated by using the combined MME/ERA method, since averaging of

multiple sets of data is not needed. This is an important aspect due to the difficulty of obtaining multiple sets of experimental data for orbiting space structures.

The finite-element model provides a fairly accurate representation of the frame at the lower modes as compared to averaged frequency Fourier responses (see Figures 4 and 5). However, the higher modes are not modeled accurately. The ERA method is effective for developing accurate state-space models when noise levels are low in nature. However, difficulties arise when higher noise levels are present in the output measurements. These effects can make a minimal state-space model of a MIMO system extremely difficult to obtain. For the identification of the testbed the ERA is able to identify the natural frequencies and damping ratios fairly accurately at the lower modes using an average of three different time histories (see Table 1). However, one of the identified higher modes is unstable when using raw measurements. Also, the eigenvalues of the identified model varied as much as 10% when using data measured at node 15 as compared to data form node 18. Therefore, a near minimal MIMO realization of the testbed is not attainable using raw measurements implemented into the ERA.

Table 1 Poles of the Identified Model

	ERA		MME/ERA		Freq. Resp.	
Mode	ω (Hz)	ζ (%)	ω (Hz)	ζ (%)	ω (Hz)	ζ (%)
1	1.91	0.50	1.91	0.46	1.91	0.38
2	4.23	0.29	4.00	0.25	3.96	0.21
3	10.00	0.26	10.14	0.21	10.07	0.21
4	15.77	0.19	15.80	0.20	15.57	0.15
5	17.38	10.0	23.10	0.13	23.14	0.11
6	25.02	0.18	29.67	0.17	29.50	0.16
7	29.37	0.59	37.06	0.13	37.09	0.11
8	38.56	-0.01	48.36	0.45	47.34	0.39
9	42.55	0.12	49.00	0.36	49.10	0.33
10	52.50	0.01	54.55	0.25	54.35	0.26
11	55.37	0.22	56.08	0.27	56.20	0.25
lights	60.00	0.00	60.00	0.00	60.00	0.00
real	0.43	100	0.20	100	0.06	100

Figure 4 Experimental, Analytical, and Identified Magnitude Plots (1st input)

Figure 5 Experimental, Analytical, and Identified Magnitude Plots (2nd input)

By combining the ERA with the MME estimator, which utilizes the minimal state-space MIMO finite-element model, improved modal identification is achieved with near minimal MIMO realizations. Plots of the estimated and measured output of node 18, excited from each of the input struts, are shown in Figures 6 and 7. From these plots, the MME algorithm is able to accurately estimate the measured data. Similar results are also obtained for estimates of output sequences at node 15. Also, plots of the first two state estimates given by the MME algorithm are shown in Figures 8 and 9. Since the finite-element model is converted to modal form, the state estimates depict the corrected (updated) modes of the structure. All of the state estimates and output estimates are used in the ERA in order to develop a MIMO realization.

Magnitude Bode plots of the MME/ERA identification results are compared to experimental frequency response characteristics in Figures 4 and 5. The MME/ERA produced a near minimal realization (24^{th} order) for the first eleven modes. A complete minimal realization is not possible since an extra mode, occurring at node 15 only, is measured between the fifth and sixth mode (see bottom graphs of Figures 4 and 5). These MIMO modeling errors could be produced by nonlinear effects acting on the test structure. However, the MIMO model produced by the integrated MME/ERA algorithm is extremely accurate with good agreement to experimental frequency response results (see Table 1). Also, the modal amplitude coherence (MAC) factors (Juang and Pappa, 1985) are also improved using the integrated algorithm. MAC factors estimate the degree of excitation, with 1 indicating full modal identification. From Table 2, the integrated algorithm shows improvements in nearly all MAC factors in the first eleven modes. Therefore, the integrated algorithm provides enhanced modal identification coupled with near minimal realizations of the complex MIMO structure.

Table 2 Modal Amplitude Coherence Factors

	MAC	
Mode	ERA	MME/ERA
1	0.9767	0.9987
2	0.9564	0.9943
3	0.9673	0.9954
4	0.9325	0.9934
5	0.8835	0.9976
6	0.9123	0.9899
7	0.7546	0.9976
8	0.0143	0.9643
9	0.2456	0.9788
10	0.6643	0.9934
11	0.6783	0.9945
lights	1.00	1.00
real	0.8653	0.9967

Figure 6 Estimated and Measured Output of Node 18 (1st input)

Figure 7 Estimated and Measured Output of Node 18 (2nd input)

Figure 8 Estimated State Time History of Mode 1 from MME (1st input)

Figure 9 Estimated State Time History of Mode 2 from MME (1st input)

Conclusions

In this paper, a robust integrated estimation/identification algorithm was developed for accurate modal realizations. This algorithm combined the Minimum Model Error estimator, using second-order analytical models, with the Eigensystem realization algorithm in order incorporate state and output estimates for the identification of system models. The unique use of second-order finite-element models enabled the MME algorithm to estimate output sequences that are a linear function of the state estimates. Also, since state estimates are integrated into the identification algorithm, averaging of multiple test runs was not required. Therefore, complex multi-input-multi-output systems can be accurately identified. The

integrated algorithm was used to develop a realization of an actual test structure from experimental data. Band-limited random noise inputs where used to excite the first eleven modes of the structure. Results indicated that the utilization of raw measurements produced inaccurate modal identification of higher modes using ERA. Also, a near minimal realization of the MIMO was not possible. However, the integrated algorithm accurately identified all modes and produced a near minimal MIMO realization of the test structure.

Acknowledgments

The authors wish to express their gratitude to Dr. Daniel J. Inman and Donald J. Leo (Department of Engineering Science and Mechanics, Virginia Polytechnic Institute and State University), for their suggestions, valuable time for the use of structural facilities at the Mechanical Systems Laboratory (MSL), and for contributing the analytical finite-element model and experimental data used in this paper.

References

Astrom, K.J., and Eykhoff, 1971, "System Identification–A Survey," *Automatica*, Vol. 7, pp. 123–162.

Bode, H.W., and Shannon, C.E., 1950, "A Simplified Derivation of Linear Least Square Smoothing and Prediction Theory," *Proceedings IRE*, Vol. 38, pp. 417–425.

Freund, J.E., and Walpole, R.E., 1987, *Mathematical Statistics*, Prentice-Hall, NJ.

Hashemipour, H.R., and Laub, A.J., 1988, "Kalman Filtering for Second-Order Models," *AIAA Journal of Guidance, Control and Dynamics*, Vol. 11, No. 2, pp. 181–186.

Heylen, W., 1990, "Optimization of Model Matrices by Means of Experimentally Obtained Dynamic Data," *Proceedings of the 8th International Modal Analysis Conference*, pp. 32–38.

Ibrahim, S.R., and Mikulcik, E.C., 1977, "A Method for the Direct Identification of Vibration Parameters from the Free Response," *Shock and Vibration Bulletin*, No. 47, Pt. 4, pp. 183–198.

Iliff, K.W., and Maine, R.E., 1984, "More Than You May Want to Know About Maximum Likelihood Estimation," *Proceedings of the AIAA Atmospheric Flight Mechanics Conference*, AIAA, New York, pp. 1–25.

Inman, D.J., 1989, *Vibration with Control, Measurement, and Stability*, Prentice-Hall, NJ.

Juang, J.-N., and Pappa, R.S., 1985, "An Eigensystem Realization Algorithm [ERA] for Modal Parameter Identification and Model Reduction," *AIAA Journal of Guidance, Control and Dynamics*, Vol. 8, No. 5, pp. 620–627.

Juang, J.-N., and Phan M., 1992, "Robust Controller Designs for Second-Order Dynamic Systems: A Virtual Passive Approach," *AIAA Journal of Guidance, Control and Dynamics*, Vol. 15, No. 5, pp. 1192–1198.

Kalman, R.E., 1960, "A New Approach to Linear Filtering and Prediction Problems," *Transactions of the ASME, Journal of Basic Engineering*, Series D, Vol. 82, pp. 34–45.

Leo, D.J., and Inman, D.J., 1992, "Control of a Flexible Frame in Slewing," *Proceedings of the American Control Conference*, Chicago, IL.

Leuridan, J.M., and Vold, H., 1983, "A Time Domain Linear Model Estimation Technique for Multiple Input Modal Analysis," *Modal Testing and Model Refinement*, ed D Chu ASME-AMD, Vol. 59, pp. 51–62.

Minas, C., and Inman, D.J., 1990, "Matching Finite Element Models to Modal Data," *ASME Journal of Vibration, Acoustics, Stress, and Reliability*, Vol. 112, No. 1, pp. 84–92.

Mook, D.J., and Junkins, J.L., 1988, "Minimum Model Error Estimation for Poorly Modeled Dynamic Systems," *AIAA Journal of Guidance, Control and Dynamics*, Vol. 11, No. 3, pp. 256–261.

Mook, D.J., and Lew, J.S., 1988, "A Combined ERA/MME Algorithm for Robust System Realization/Identification," *Proceedings of the 29th Structures, Structural Dynamics, and Materials Conference (S.D.M.)*, Williamsburg, Virginia.

Roemer, M.J., and Mook, D.J., 1990, "An Enhanced Mode Shape Identification Algorithm," *Proceedings of the 30th Structures, Structural Dynamics, and Materials Conference (S.D.M.)*, Mobile, Alabama.

Roemer, M.J., and Mook, D.J., 1992, "Robust Modal Identification/Estimation of the Mini-Mast Testbed," *AIAA Journal of Guidance, Control and Dynamics*, Vol. 15, No. 3, pp. 642–647.

Smith, W.R., 1981, "Least Square Time Domain Method for Simultaneous Identification of Vibration Parameters from Multiple Free Response Records," *AIAA Paper*, #81–0530.

Vaughan, D.R., 1970, "A Nonrecursive Algebraic Solution for the Discrete Riccati Equation," *IEEE Transactions on Automatic Control*, Vol. AC-15, pp. 597–599.

Weiner, N., 1949, *Extrapolation, Interpolation and Smoothing of Stationary Time Series, with Engineering Applications*, Technology Press and Wiley, New York.

Yeh, F.B., and Yang, C.D., 1987, "New Time Domain Identification Technique," *AIAA Journal of Guidance, Control and Dynamics*, Vol. 10, No. 3.

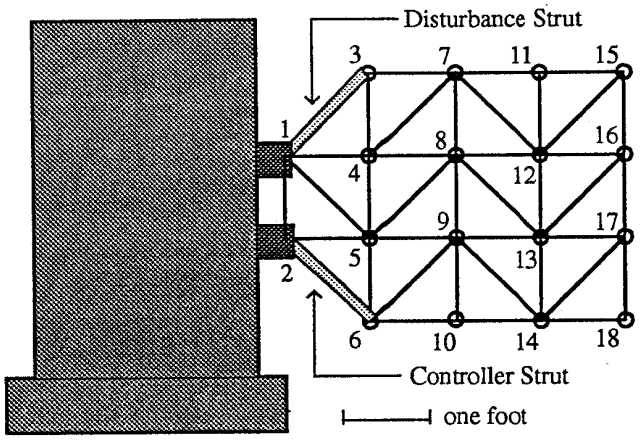
Disturbance Strut
3
7
11
15
1
8
16
4
12
9
17
5
13
2
6
10
14
18
Controller Strut
one foot

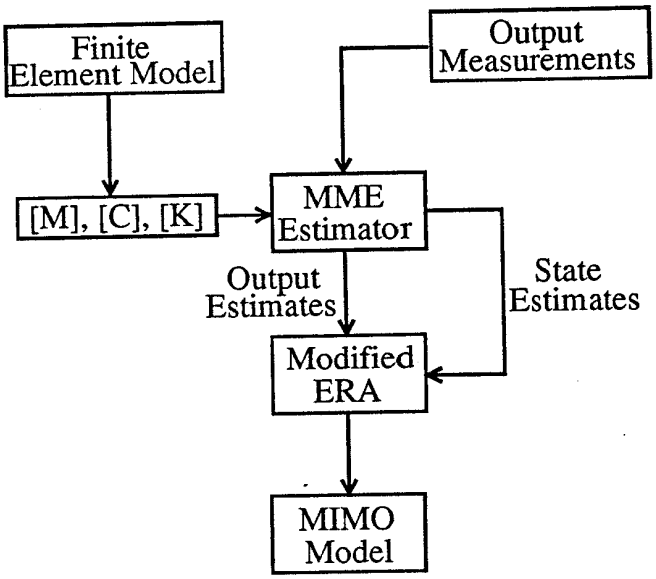
Finite Element Model
Output Measurements
[M], [C], [K]
MME Estimator
Output Estimates
State Estimates
Modified ERA
MIMO Model

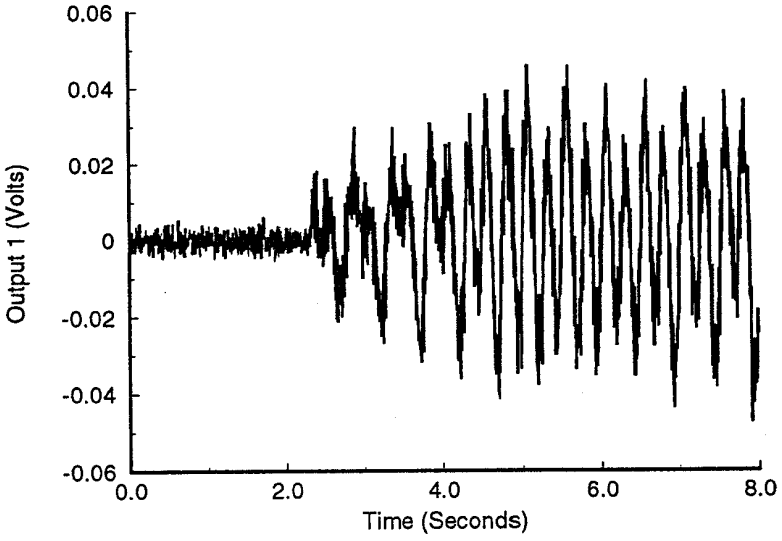
0.06
0.04
0.02
0
-0.02
-0.04
-0.06
Output 1 (Volts)
0.0
2.0
4.0
6.0
8.0
Time (Seconds)

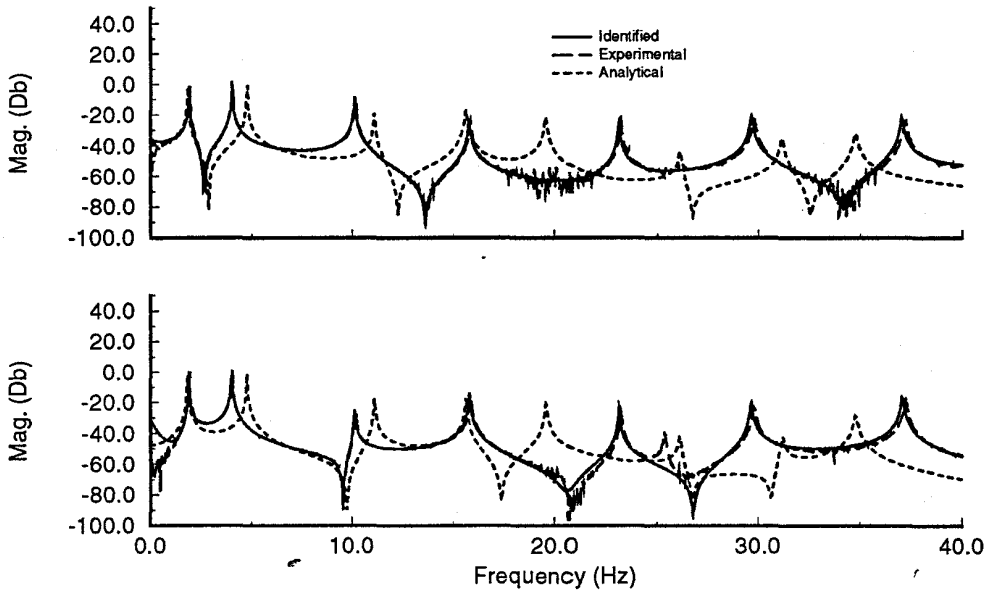
Identified
Experimental
Analytical
Mag. (Db)
40.0
20.0
0.0
-20.0
-40.0
-60.0
-80.0
-100.0
Mag. (Db)
40.0
20.0
0.0
-20.0
-40.0
-60.0
-80.0
-100.0
0.0
10.0
20.0
30.0
40.0
Frequency (Hz)

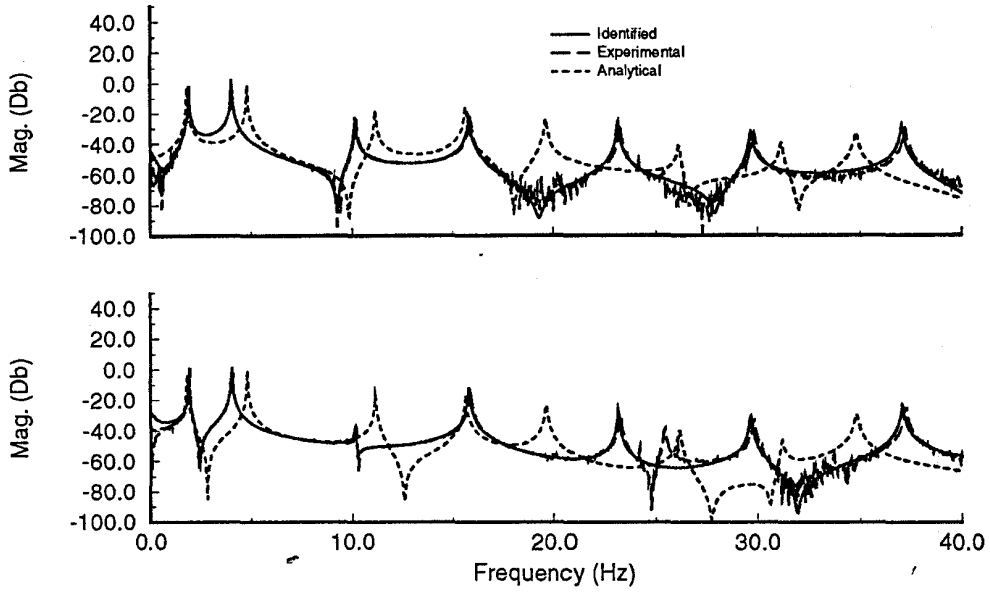
Identified
Experimental
Analytical
Mag. (Db)
40.0
20.0
0.0
-20.0
-40.0
-60.0
-80.0
-100.0
Mag. (Db)
40.0
20.0
0.0
-20.0
-40.0
-60.0
-80.0
-100.0
0.0
10.0
20.0
30.0
40.0
Frequency (Hz)

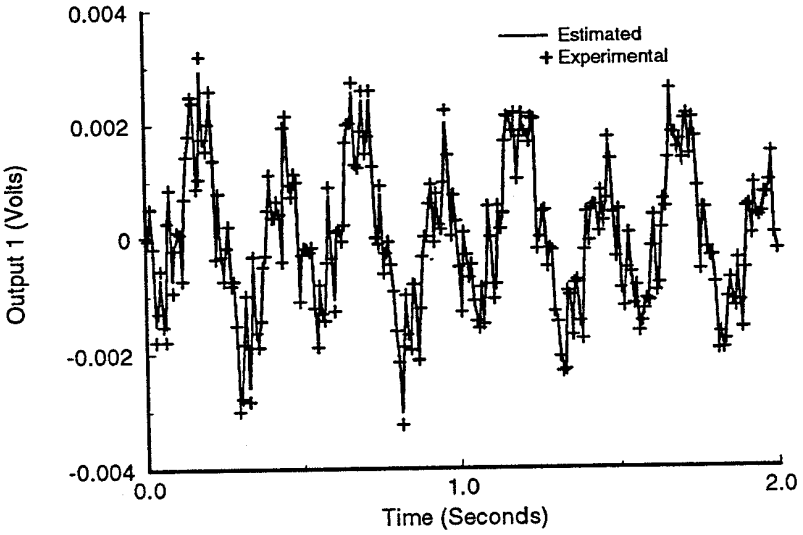
0.004
0.002
0
-0.002
-0.004
0.0
1.0
2.0
Output 1 (Volts)
Time (Seconds)
Estimated
Experimental

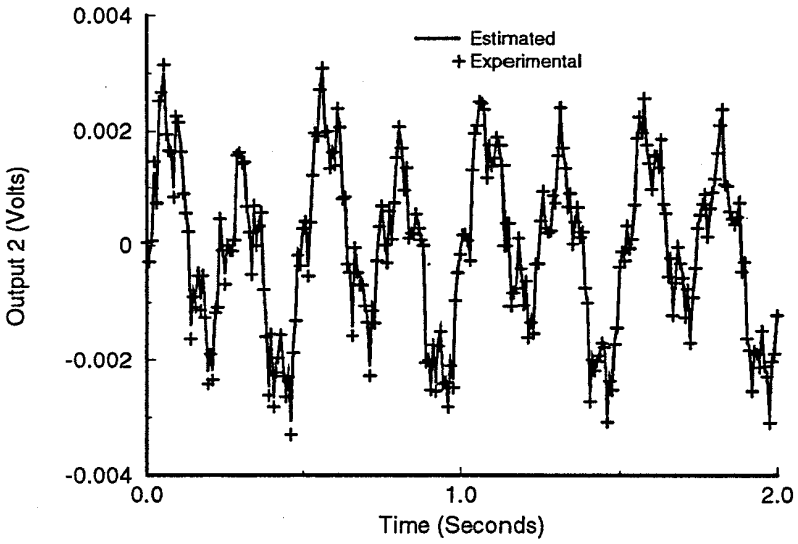
0.004
0.002
0
-0.002
-0.004
0.0
1.0
2.0
Output 2 (Volts)
Time (Seconds)
Estimated
+ Experimental

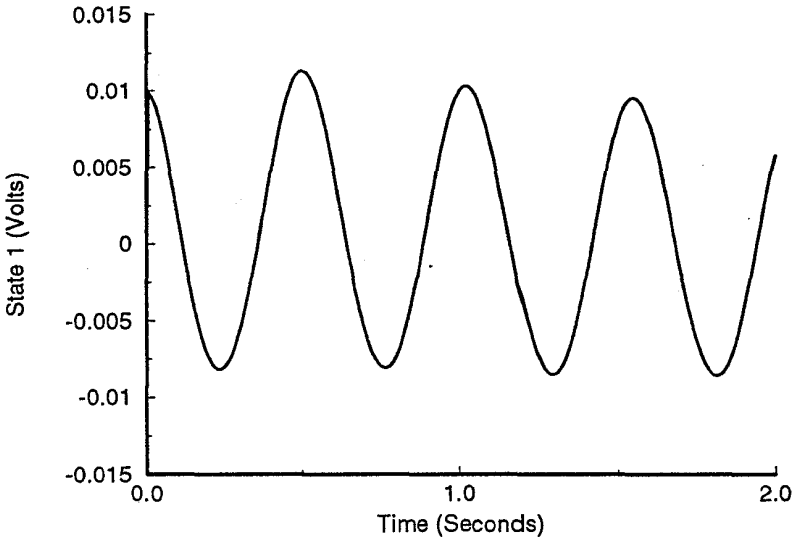
0.015
0.01
0.005
0
-0.005
-0.01
-0.015
State 1 (Volts)
0.0
1.0
2.0
Time (Seconds)

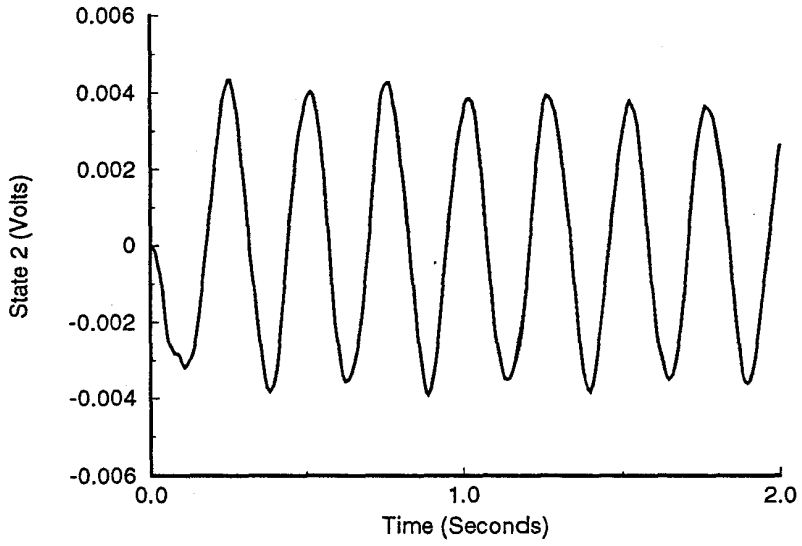
0.006
0.004
0.002
0
-0.002
-0.004
-0.006
State 2 (Volts)
0.0
1.0
2.0
Time (Seconds)